J Mol Model (2013) 19:589–599
DOI 10.1007/s00894-012-1576-z

ORIGINAL PAPER

Hydrogen bonds in galactopyranoside and glucopyranoside: a density functional theory study

Zahrabatoul Mosapour Kotena · Reza Behjatmanesh-Ardakani · Rauzah Hashim · Vijayan Manickam Achari

Received: 18 May 2012 / Accepted: 20 August 2012 / Published online: 13 September 2012

Abstract Density functional theory calculations on two glycosides, namely, *n*-octyl-β-D-glucopyranoside (C_8O-β-Glc) and *n*-octyl-β-D-galactopyranoside (C_8O-β-Gal) were performed for geometry optimization at the B3LYP/6-31G level. Both molecules are stereoisomers (epimers) differing only in the orientation of the hydroxyl group at the C4 position. Thus it is interesting to investigate electronically the effect of the direction (axial/equatorial) of the hydroxyl group at the C4 position. The structure parameters of X-H···Y intramolecular hydrogen bonds were analyzed, while the nature of these bonds and the intramolecular interactions were considered using the atoms in molecules (AIM) approach. Natural bond orbital analysis (NBO) was used to determine bond orders, charge and lone pair electrons on each atom and effective non-bonding interactions. We have also reported electronic energy and dipole moment in gas and solution phases. Further, the electronic properties such as the highest occupied molecular orbital, lowest unoccupied molecular orbital, ionization energy, electron affinity, electronic chemical potential, chemical hardness, softness and electrophilicity index, are also presented here for both C_8O-β-Glc and C_8O-β-Gal. These results show that, while C_8O-β-Glc possess– only one hydrogen bond, C_8O-β-Gal has two intramolecular hydrogen bonds, which further confirms the anomalous stability of the latter in self-assembly phenomena.

Keywords Atoms in molecules theory · Density functional theory · Glycolipids · Hydrogen bonding · Natural bond orbital analysis

Z. Mosapour Kotena (✉) · R. Hashim · V. Manickam Achari
Chemistry Department, Faculty of Science, University of Malaya, 50603, Kuala Lumpur, Malaysia
e-mail: zahrabatool2@siswa.um.edu.my

R. Behjatmanesh-Ardakani
Department of Chemistry, Payame Noor University, PO BOX 19395-3697, Tehran, Iran

Introduction

Glycopyranoside is a family of non-ionic surfactants from the more generic class of glycolipids found in nature, especially in biological membranes [1, 2]. These molecules have an amphiphilic nature, comprising a sugar part which is highly polar and hydrophilic, and a lipid moiety–usually involving alkyl-chain, which is non-polar and hydrophobic. The dichotomy of forces, in this case the hydrophilic and hydrophobic (water hating/water liking), not only generates polarity difference within the molecule, but also induces a microphase separation between the two regions. Thus, these molecules self-assemble into several possible mesophases, depending on factors such as temperature and composition [3, 4]. The self-assembling nature of these molecules is of interest to many industries like food and pharmaceuticals, [5] and they have been used widely as emulsifiers to stabilize suspended food mixtures or as drug carriers with an added advantage of their nontoxic and biodegradable nature [6, 7].

One widely-studied sugar-based surfactant is n-octly-β-D-gluctopyranoside (C_8O-β-Glc) [8, 9]. It has been used for a variety of applications, from being a stabilizer, reconstituting, purifying and crystallizing membrane proteins and membrane-associated protein complexes without denaturation [10, 11], to being used in molecular recognition and cell signaling [12]. Therefore, understanding its interactions among the constituent molecules is of special interest. In principle, molecular interactions contribute much in determining the formation of mesophases. Most notably, the hydrophobic region is mainly governed by the non-bonded van der Waals force, whereas within the hydrophilic region, the long range electrostatic interaction from the hydroxyl group plays a vital role. Additionally, distance- and direction-orientated hydrogen bonding interaction within the hydrophilic domain determines the thermodynamic stability of the self-assembly structure [13, 14].

In principle, a hydrogen bond (HB) occurs in between a proton donor (H) attached covalently to a highly electronegative atom, for example –OH group and a proton acceptor (O), which has two lone pairs of electrons. It has been categorized as a middle range interaction, which falls in between the weak van der Waals interaction and the strong covalent or ionic interactions. In general, this bond has an energy value range from as low as 0.24–0.28 kcalmol^{-1} (for weak hydrogen bond) and this value could reach up to a maximum value of 38 kcalmol^{-1}. On average most HB ranges are between 1.2 and 7.2 kcalmol^{-1} [15–17]. This wide range of energy value for hydrogen bond is highly expected to allow for many diverse behaviors of biomolecules and play many dominant roles in chemical reactions and self-assembly [18, 19]. In the context of the sugar groups the water-carbohydrate bond energies are in the range of approximately 3.34–6.45 kcalmol^{-1} and could become as low as 1.2 kcalmol^{-1} if cooperative effect comes into play [20]. For a system such as maltose with eight hydroxyl groups (OHs), the intra and intermolecular hydrogen bonds between the sugar groups and the solvent play a crucial role in determining the behavior of the conformations [19, 21, 22]. The strength of these hydrogen bonds allows for strong resistance to thermal distortion of the structure at room temperature, which is about a magnitude higher than *kT*. Thus, the conformation of sugar and their solvation properties is influenced by the presence of the HB [21]. The physico-chemical properties of sugars such as melting and clearing temperatures are primarily affected by the directionally oriented hydrogen bonding. A similar behavior is expected of the monosaccharide groups present within glycolipids such as n-octyl-β-D-glucopyranoside (C_8O-β-Glc) and n-octyl-β-D-galactopyranoside (C_8O-β-Gal). The hydrophilic region contains four OHs, involved in inter- and intramolecular hydrogen bonding. In the molecular dynamic simulation study of these systems by Chong et al. [22], it was found that the thermal stability of the self-assembly structure was related to the intralayer instead of the interlayer hydrogen bonds. These results were far from being conclusive and a more detailed calculation is necessary to establish this relationship.

There are many definitions for a hydrogen bond and these have been reviewed recently [23]. Here, we use the definition as suggested by Bader, since atom in molecule (AIM) theory [24] was applied to understand in greater detail the nature of HBs. Excellent reviews have been published [24–26] on the applications of AIM for such calculations. Within AIM, the analysis of the bond critical points (BCP) on the electronic density distribution has proven useful in the study of different chemical features such as the structure, nature and geometry of hydrogen-bonded systems [27–29].

In general, for carbohydrate monomer, the ring puckering and the multiple bonding sites for primary and secondary hydroxyl groups contribute many conformational preference observables, which in turn helps in stable structure prediction [30]. To understand the complex conformational spaces, a systematic study at the rotors, specifically at glycosidic bonds between monomers and linkage at hydroxymethyl groups provides meaningful expositions for the flexibility shown by a monomer. The hydroxymethyl group (primary alcohol) has three staggered rotamers about the O5-C5-C6-O6 dihedral angle namely, gauche-gauche (gg), gauche-trans (gt) and trans-gauche (tg) [31]. A recent computational study has shown that gauche effect in sugar monomers determines the conformation of gg, gt and tg population in both vacuum and explicit water environments. In glucose moiety, gg conformer is the most preferred in vacuum compared to gt and tg conformers, but in the presence of water, the preference changes in the order of gt > gg > tg. A similar trend as that shown by the galactose is observed where the ordering of hydroxymethyl population changes from gt > gg > tg in vacuum to gt > tg > gg in water environment. This can be explained by the existence of intramolecular hydrogen bonding among the hydroxyl groups and bridging hydrogen bonds with water molecules due to the change in conformer populations [31].

Interestingly, an *ab initio* study by Grabowski [32] gives an inverse proportional relationship between distance of (OH ···O) and (O-H) bond strength. When the HB is stronger, the length of O-H bond becomes greater but the H···O and O···O distances are shorter and these results do agree with those from previous studies [33, 34].

The knowledge of the nature of hydrogen bond is most important due to its crucial role in different biological processes. In membrane science, for example, the subtle difference between glucolipid and its epimer galactolipid have shown profound impact on the cell functions. While galactolipids are pervasively found in plant cells, its epimer glucolipids are usually found in bacteria [35]. The formers are thought to be involved in photosynthesis. This suggests a hydroxyl group with a different orientation (equatorial/axial) on the sugar ring gives different degree of hydrogen bonding interaction. Thus, our interest in the present investigation reflects this concern. The aim of the present study is to analyze the intramolecular OH O hydrogen bonds for C_8O-β-Glc (Fig. 1a) and C_8O-β-Gal (Fig. 1b), to get an insight into their detailed bonding nature. To acheive this aim, on density functional theory (DFT) was used to calculate the equilibrated geometry of these structures and AIM approach was used to characterize the nature of the intramolecular hydrogen bonds. Useful parameters such as electronic density $\rho(r)$, at the bond critical point and, its Laplacian $\nabla^2\ \rho(r)$, is used for estimating the strength of the hydrogen bond [36]. The natural bond orbital

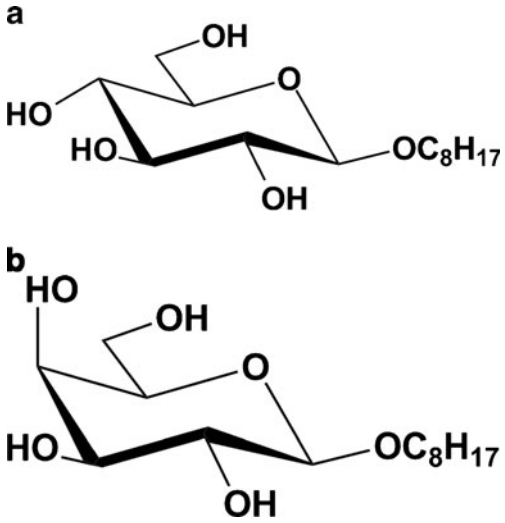

Fig. 1 Schematic drawings of molecular structures for (**a**) C_8O-β-Glc and (**b**) C_8O-β-Gal

(NBO) analyses [37, 38] of decomposition was applied to analyze the charge transfer effect on the OH O interaction of the calculated data.

Computational methods and details

Three methods were used for the investigation of intramolecular hydrogen bonding interaction in C_8O-β-Glc and C_8O-β-Gal namely; DFT, AIM theory and NBO analysis. An efficient and widely used technique to study a molecular structure, DFT, with B3LYP/6-31G level of calculation was applied to optimize the molecules under investigation, (C_8O-β-Glc and C_8O-β-Gal), both in gas and solution phases. The B3LYP (Becke-Lee-Yang-Parr) version of DFT is the combination of Becke's three-parameter non-local hybrid functional of exchange terms [39] with the Lee, Yang and Parr correlation functional [40]. The basis set 6–31 G contains a reasonable number of basis set functions that are able to reproduce experimental data [41, 42]. The solution phase was studied by polarizable continuum model (PCM) [43]. All calculations were performed using Gaussian 09 software package [44]. Gauss View 5.0. [45] was used to prepare the input file and to visualize the optimized structures. Using the DFT method, the best minimum energy conformations were achieved by full geometry optimization of each glycolipids. In order to prove that each of them is located at a stable minimum point of the potential energy surface, frequency calculations were carried out based on these optimized structures and subsequently obtain their vibration frequencies. Furthermore, using the results obtained from the calculation, the structural and electronic properties such as ionization potentials *(I)*, HOMO energies ε_{HOMO}, LUMO energies ε_{LUMO}, bond length, electron affinity (*A*), chemical hardness (η), electronic chemical potential (μ), electrophilicity index (ω), were investigated. The topological parameters such as electron densities $\rho(r)$, and their Laplacians $\nabla^2\ \rho(r)$, at BCP were obtained from the Bader theory [46, 47] by using AIM 2000 software [48]. The nature of intramolecular interactions of C_8O-β-Glc and C_8O-β-Gal was investigated by using the NBO 3.1 package [49].

Results and discussion

Energies and geometries

Figure 2 defines the hydrogen bonding geometry based on Jeffrey and Saenger [18], and other related properties to this definition are presented in Table 1 [50, 51]. This table shows general characteristics of strong, moderate and weak hydrogen bonds. Strong hydrogen bond interaction is partially covalent; for a moderate one this involves mostly electrostatic, while a weak hydrogen bond involves electrostatic or dispersed interaction. In addition, it should be noted that the normal covalent bond length is about 0.96 Å, while that of the intramolecular hydrogen bonding in the carbohydrate moiety is in the range of 1.8−2.6 Å [18].

The optimized geometries of both pyranosides at the B3LYP/6-31G level of theory are shown in Fig. 3. The bond lengths and bond angles of C_8O-β-Glc and C_8O-β-Gal values are given in Table 2. The four normal bond lengths of hydroxyl groups (refer to Fig. 3 for atom lables) are O2-HO2, O3-HO3, O4-HO4 and O6-HO6 have values of about 0.97±0.01 Å.

From AIM (see later discussion), an extra intramolecular hydrogen bond of HO6···O4 for C_8O-β-Glc is observed. On the other hand, for C_8O-β-Gal two extra bonds are observed corresponding to HO6···O4 and HO6···O4. These intramolecular hydrogen bonds are expected to be weaker than the normal covalent O-H. The optimized HO6···O4 bond length in C_8O-β-Glc is about 2.11 Å. For C_8O-β-Gal, the values of the two optimized hydrogen bonds (HO6···O4 and HO6···O3) are 1.85 Å and 2.09 Å, respectively. These

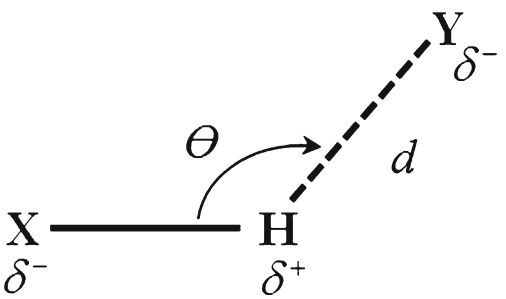

Fig. 2 Definition of HB geometry where the angle of hydrogen bonding of X-H···Y, θ , and hydrogen bond distance, d, [18]

Table 1 General characteristic of the three major types of hydrogen bonding and important structural parameters) [18, 50, 51]

Interaction type	Strong Partially covalent	Moderate Mostly electrostatic	Weak Electrostatic / dispersed
Bond lengths (Å) H···Y	1.2–1.5	1.5–2.2	2.2–3.3
Lengthening of X-H (Å)	0.08–0.25	0.02–0.08	<0.02
X-H vs H···Y	X-H ≈ H···Y	X-H < H···Y	X-H < < H···Y
X···Y(Å)	2.2–2.5	2.5–3.2	>3.2
Directionality	strong	moderate	Weak
Bond angles(°)	170–180	>130	>90
Bond energy(kcal mol^{-1})	> 8	4–8	<4

distances are similar to those found for other sugar intramolecular hydrogen bonding. For example, the calculated values for pentahydrates of α- and β-D-glucopyranose [54], α- and β-D-mannopyranose [55], and α- and β-D-galactopyranose [52] range from 2 to 3 Å. The O6-HO6-O4 angle in both C_8O-β-Glc and C_8O-β-Gal are 127° and 140°, respectively. However, the O4-HO4-O3 angle in the C_8O-β-Gal is 114°. The results are in accord with the experimental data [18].

The calculated electronic energies of C_8O-β-Glc and C_8O-β-Gal, both at the B3LYP/6-31G level of theory in the gas and solution phases (water solvent), are summarized in Table 3. The results show that C_8O-β-Gal is more stable than C_8O-β-Glc in both gas and solution phases. The differences in electronic energies between C_8O-β-Gal and C_8O-β-Glc in the gas and solution phases are -1.6 kcal mol^{-1} and −3.0 kcal mol^{-1} respectively, indicating that both C_8O-β-Gal and C_8O-β-Glc are more stable in the solution phase than in the gas phase. Additionally, the electronic energy difference for the C_8O-β-Glc in PCM and gas phases and that of C_8O-β-Gal are −10.3 kcal mol^{-1} and −11.7 kcal mol^{-1} respectively, implying that C_8O-β-Gal is more stable than C_8O-β-Glc. The dipole moment analysis in the gas phase and PCM is given in Table 3. Dipole moment in the C_8O-β-Gal is more than in C_8O-β-Glc in both gas and PCM phases. Differences in dipole moment between the two compounds in the gas phase and PCM are 0.38 and 1.4 Debye respectively, and the ratio for C_8O-β-Gal is three times more than that for C_8O-β-Glc. This ratio value is in accordance with the calculated results for water by Silvestrelli and Parrinello [56].

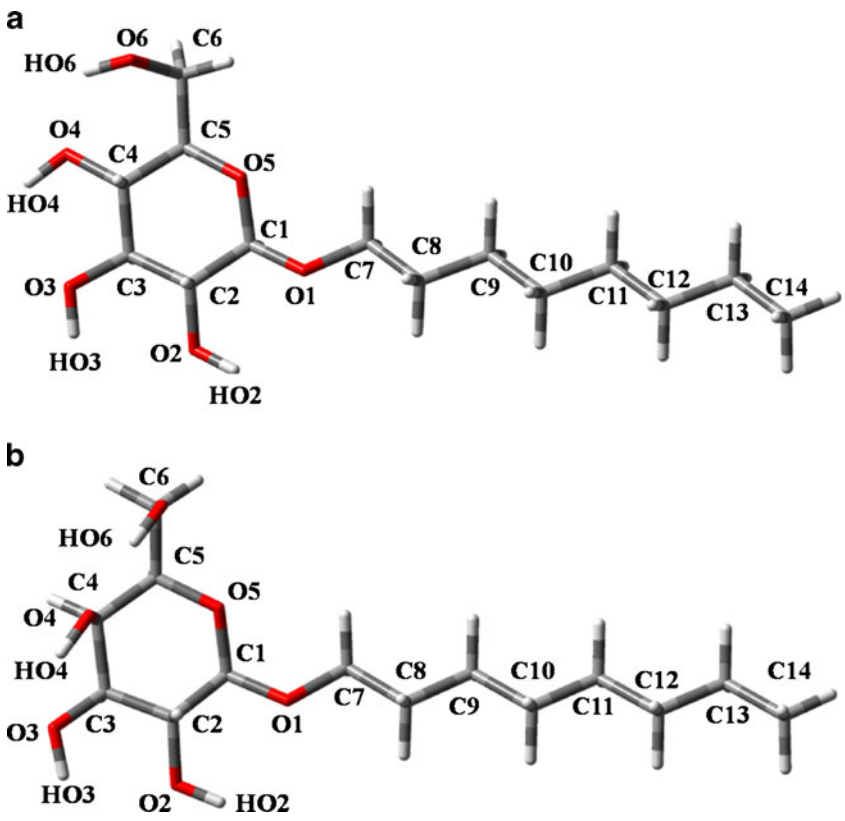

Fig. 3 The optimized structure at the level of theory B3LYP/6-31G for **a** C_8O-β-Glc and **b** C_8O-β-Gal. The IUPAC naming convention for carbohydrate is used for labeling the atoms [53]

Table 2 The geometrical parameters for C_8O-β-Glc and C_8O-β-Gal (the bonds in Å and the angles in degree), at the B3LYP/6-31G by DFT method. For the atom labels we used Mamony et al. [52] and IUPAC [53]

	C_8O-β-Glc	C_8O-β-Gal
Covalent bond length (Å)		
O2-HO2	0.97	0.97
O3-HO3	0.97	0.97
O4-HO4	0.98	0.98
O6-HO6	0.98	0.98
Hydrogen bond length (Å)		
HO4···O3	–	2.09
HO6···O4	2.11	1.85
Hydrogen bond angle (°)		
O4-HO4···O3	–	114
O6-HO6···O4	127	140

Table 4 lists the electronic properties of C_8O-β-Gal and C_8O-β-Glc, including energy of the highest occupied molecular orbital (ε_{HOMO}), and energy of the lowest unoccupied molecular orbital (ε_{LUMO}), ionization energy (I), electron affinity (A), chemical hardness (η), electronic chemical potential (μ), electrophilicity index (ω), and softness (S). Parr et al. [57] have defined electrophilicity index (ω), as a new descriptor to quantify the global electrophilic nature of a molecule within a relative scale. This index measures the stabilization in energy when the system acquires an additional electronic charge from the environment. The small value of electrophilicity index (ω), indicates that the molecule is stable. Chemical potential (μ), chemical hardness (η), and softness (S), are known as global reactivity descriptors [58–60]. Global hardness and softness are of interest, since resistance to change of the electron cloud of the chemical system can be understood from the values of hardness (η), and softness (S). The stability of chemical species can be associated with its hardness. Hard molecules have a large energy gap between (ε_{LUMO}) and (ε_{HOMO}) and soft molecules have a small one [61, 62]. It can be readily seen from Fig. 4, that the gap for C_8O-β-Glc is 0.49659 eV, which is higher than that for C_8O-β-Gal 0.47510 eV,

Table 3 Electronic energy, E (a.u.) and dipole moment, μ(D), of studied compounds at B3LYP/6-31 G level of theory in the gas and solution phases

	E (a.u.)[a]		μ (D)[b]	
	Gas phase	PCM	Gas phase	PCM
C_8O-β-Glc	−1001.36598	−1001.38236	4.011	4.231
C_8O-β-Gal	−1001.36851	−1001.38709	4.390	5.609

[a] in atomic unit. 1 a.u. is equal to 627.5095 kcalmol^{-1}

[b] in Debye

indicates C_8O-β-Glc is hard specie and C_8O-β-Gal is soft specie. A comparison of reactivity descriptors in Table 4 also indicates that C_8O-β-Glc is harder than C_8O-β-Gal. Because of the inverse relationship between the hardness and stability, C_8O-β-Gal is reactive specie when compared to C_8O-β-Glc. As shown in Table 4, the electronphilicity values for C_8O-β-Glc and C_8O-β-Gal are 0.00138 and 0.00089, respectively. The smaller value of electrophilicity for C_8O-β-Gal indicates that C_8O-β-Gal is more stable than C_8O-β-Glc. This further implies that C_8O-β-Glc is less likely to associate itself with electrons from the surroundings compared to C_8O-β-Gal. After all, the latter has two intramolecular hydrogen bonds, as seen from AIM analysis.

Atoms in molecules analysis

Bader's theory of atoms in molecules [63] is widely used as a theoretical tool to understand and analyze hydrogen bonds. The formation of HB is associated with the appearance of a BCP between the hydrogen atom of donor group and acceptor. This theory is based on the critical points (CPs) of the molecular electronic charge density $\rho(r)$. At these points, where the density gradient $\nabla\rho(r)$, vanishes are characterized by the three eignvalues ($\lambda_{i,i=1,2,3}$), of the Hessian matrix. λ_1 and λ_2 correspond to the perpendicular curvatures, while λ_3 provides a curvature along the internuclear axis. The CPs are labeled (r,s), according to their rank r (number of non-zero eignvalues), and signatures s, (the algebraic sum of the signs). Four types (r,s) of CPs are of interest in molecules and these are (3,+3), (3,+1), (3,−3), (3,−1). In our case a (3,−1) point or bond critical point is generally found between two neighboring nuclei indicating the existence of a bond between them.

Popelier and Bader [64] employed the AIM analysis to address several important chemical issues [65] where he proposed a set of criteria for the existence of hydrogen bonding within the AIM formalism. Two of these criteria are related to electron density $\rho(r)$, and the Laplacian of the electron density $\nabla^2\rho(r)$, evaluated at the bond critical point (BCP) of two hydrogen bonded atoms. In general, if hydrogen bond exists, the range of $\rho(r)$ and $\nabla^2\rho(r)$ are 0.002–0.035 and 0.024–0.139 a.u., respectively [64]. We have tabulated the topological parameters collected in Table 5. It is evident from this table that the values of $\rho(r)$ and $\nabla^2\rho(r)$ in the C_8O-β-Glc, in HO6···O4 interaction are 0.0209 and 0.0730 a.u, respectively. However, in the C_8O-β-Gal, HO6···O4 and HO4···O3 interaction are 0.0332, 0.0217 and 0.1217, 0.0839 a. u, respectively. These characteristic electron densities at BCP imply the presence of hydrogen bonding interaction.

The Laplacian of charge density at the bond critical point, $\nabla^2\rho(r)$, is the sum of the curvatures in the charge density

Table 4 Calculated highest occupied molecular orbital ε_{HOMO} and lowest unoccupied molecular orbital ε_{LUMO}, energies, ionization energy (I), electron affinity (A), chemical hardness (η), electronic chemical potential (μ), electrophilicity index (ω), and softness (S) of C8O-β-Glc and C8O-β-Gal at the B3LYP/6-31G level

Electronic properties	Formula	C_8O-β-Glc	C_8O-β-Gal
Energy of LUMO (eV)	(ε_{LUMO})	0.22210	0.21689
Energy of HOMO (eV)	(ε_{HOMO})	−0.27449	−0.25821
Ionization energy (eV)	$I=-(\varepsilon_{HOMO})$	0.27449	0.25821
Electron affinity (eV)	$A=-(\varepsilon_{LUMO})$	−0.22210	−0.21689
Chemical hardness (eV)	$\eta=\frac{(I-A)}{2}$	0.24829	0.23755
Electronic chemical potential (eV)	$\mu=\frac{-(I+A)}{2}$	−0.02619	−0.02066
Electrophilicity index (eV)	$\omega=\frac{\mu^2}{\eta}$	0.00138	0.00089
Softness (1/eV)	$S=\frac{1}{\eta}$	4.27467	4.20964

along any orthogonal coordinate axes at the BCP. The sign of $\nabla^2\ \rho(r)$ indicates whether the charge density is locally depleted $\nabla^2\ \rho(r)>0$, or locally concentrated $\nabla^2\ \rho(r)<0$. Thus, when the curvatures are negative, i.e., λ_1 and λ_2 dominate at the BCP, the electronic charge is locally concentrated within the region inter atoms leading to an interaction named as covalent or polarized bonds and being characterized by large $\rho(r)$, values, $\nabla^2\ \rho(r)<0$, and $\frac{|\lambda_1|}{\lambda_3}>1$. On the other hand, if the curvature is positive, i.e., λ_3 is dominant, the electronic density is locally concentrated in each of the atomic basins. The interaction is now referred to as a closed-shell and it is characteristic of highly ionic bonds, hydrogen bonds or van der Waals interactions. It is characterized by relatively low $\rho(r)$, values $\nabla^2\ \rho(r)>0$, and $\frac{|\lambda_1|}{\lambda_3}<1$ [46].

The molecular graphs (indicating critical points and bond paths) for these two molecules are shown in Fig. 5. The position of the bond critical point strongly depends on electronegativity.

The values of the electron density $\rho(r)$, its Laplacian $\nabla^2\ \rho(r)$, total energy density $H(r)$, electronic kinetic energy density $G(r)$ and electronic potential energy density $V(r)$, at BCP, are given in Table 5. For C_8O-β-Glc, the molecular graph represents one intramolecular hydrogen bond, while for C_8O-β-Gal, the molecular graph represents two intramolecular hydrogen bonds. The signs of $\nabla^2\ \rho(r)$ and $H(r)$ in the C_8O-β-Glc are positive and negative, respectively. Therefore, this bond is classified as partially covalent–partially electrostatic (Pc-Pe) [66]. In addition, the values of $\nabla^2\ \rho(r)$ and $H(r)$, in C_8O-β-Gal for the HO6···O4 interaction are positive and negative, respectively, but in the HO4···O3 interaction, they are positive. Therefore HO6···O4 interaction is partially covalent-partially electrostatic, while the HO4···O3 interaction is van der Waals. By comparing the values of $\nabla^2\ \rho(r)$, and $H(r)$, it can be concluded that the partially covalent–partially electrostatic of HO6···O4 in C_8O-β-Gal is greater than in C_8O-β-Glc, in good agreement with the smaller HO6···O4 distance calculated in the C_8O-β-Gal. The density change is due to the charge transfer from the proton acceptor to the proton donor (X-H) bond. The process increases the O-H bond length, and decreases the charge density in both C_8O-β-Glc and C_8O-β-Gal, causing the bond to be weaker. Consequently, the electrons are delocalized in the bond.

The total electron energy density $H(r)$, and the Laplacian $\nabla^2\ \rho(r)$, at BCP are two topological parameters often applied to classify and characterize hydrogen bonds. It should be mentioned that hydrogen bond is characterized by $H(r)<0$ and $\nabla^2\ \rho(r)<0$ for strong hydrogen bonds, while medium hydrogen bonds with $H(r)<0$ and $\nabla^2\ \rho(r)>0$, and $H(r)>0$, and $\nabla^2\ \rho(r)>0$ are established for weak ones [46]. From the current work, the HO-6 O-4 interaction in the C_8O-β-Glc ($\rho(r)=0.0209$, $\nabla^2\ \rho(r)=0.0730$, $H(r)=-0.0003$) and those of the C_8O-β-Gal ($\rho(r)=0.0332$, $\nabla^2\ \rho(r)=0.1217$, $H(r)=-0.0005$) are classified as medium hydrogen bonds. In addition, the HO4···O3 hydrogen bonds in the C_8O-β-Gal ($\rho(r)=0.0217$,$\nabla^2\ \rho(r)=0.0839$, $H(r)=+0.00040$) is placed in the weak hydrogen bonds category. The values of $\rho(r)$ and $\nabla^2\ \rho(r)$ at HO6···O4 bond critical points in the C_8O-β-Gal are greater than the corresponding values in the C_8O-β-Glc. On the other hand, for the HO6···O4 in the C_8O-β-Gal, the bond length is shorter than the corresponding value in the C_8O-β-Glc (see Table 2). Thus, the HO6···O4 hydrogen bond in the C_8O-β-Gal is stronger than that in C_8O-β-Glc. Furthermore, comparing two hydrogen bonds in C_8O-β-Gal, we can say that the HO6···O4 hydrogen bond is stronger than HO4···O3.

Another interesting parameter is ellipticity (ε), defined as follows:

$$\varepsilon=\left[\left(\frac{\lambda_1}{\lambda_2}\right)-1\right], \tag{1}$$

in which λ_1 and λ_2 are the curvatures of the density with respect to the two principal axes X' and Y'. It is indicative of the similarity between the perpendicular curvatures (λ_1 and λ_2)at the BCP. In terms of the orbital model of electronic structure, ellipticity provides a quantitative measure of the π-bond character and delocalization of the electronic charge. Also, ellipticity is a measure of bond stability, i.e., high ellipticity values indicate instability of the bond [24, 47].

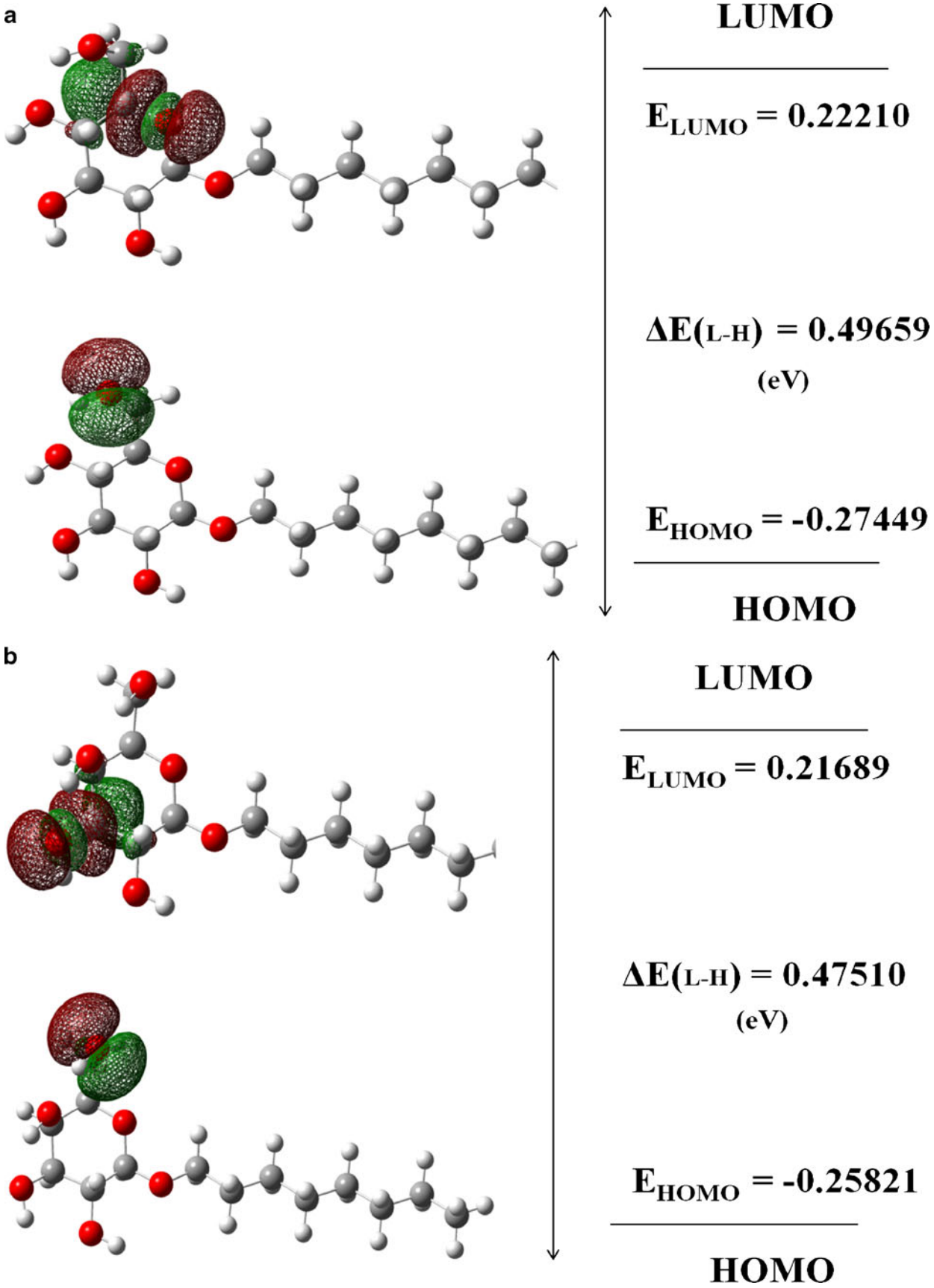

Fig. 4 The atomic orbital composition of the frontier molecular orbital for **a** C_8O-β-Glc and **b** C_8O-β-Gal

Table 5 Topological parameters (in a.u.), the electron densities $\rho(r)$, at O···H BCPs, their Laplacians $\nabla^2 \rho(r)$ and energetic parameters $V(r)$, $G(r)$ and $H(r)$ (in kcalmol^{-1}) in the C_8O-β-Glc and C_8O-β-Gal at the B3LYP/6-31G

Glycolipid	HB-length (Å)	$\rho(r)$	$\nabla^2 \rho(r)$	$V(r)$	$G(r)$	$H(r)$	Ellipticity(ε)
C_8O-β-Glc	HO6···O4=2.11	0.0209	0.0730	−0.0189	0.0186	−0.0003	0.1538
C_8O-β-Gal	HO6···O4=1.85	0.0332	0.1217	−0.0315	0.0309	−0.0005	0.0338
	HO4···O3=2.09	0.0217	0.0839	−0.0202	0.0206	+0.0004	0.3886

As Table 5 shows, ellipticity (ε) in the C_8O-β-Glc is 0.1538 a.u for the HO6···O4, while in the C_8O-β-Gal, it is 0.0338 a.u. This means hydrogen bonding in the C_8O-β-Glc is more unstable than in the C_8O-β-Gal. Ellipticity of two positions (HO6···O4, HO4···O3) in the C_8O-β-Gal is 0.0338 and 0.3886, respectively. These values show that hydrogen bonding in the HO6···O4 interaction is more stable than the bond in HO4···O3

Natural bond orbital analysis

In the NBO analysis [38], electronic wave functions are interpreted in terms of a set of occupied Lewis and a set of unoccupied non-Lewis localized orbitals. Delocalization effects can be identified from the presence of off-diagonal elements of the Fock matrix in the NBO basis. The strengths of these delocalization interactions $E^{(2)}$ are estimated by second order perturbation theory. In addition, the stabilization energy $E^{(2)}$ associated with $i \rightarrow j$ delocalization is explicitly estimated by the following equation:

$$E^{(2)} = \Delta E_{ij} = qi\frac{F(i,j)^2}{s_j - s_i}, \quad (2)$$

where q_i is the ith donor orbital occupancy ε_j, ε_i is diagonal elements (orbital energies) and F (i, j) is the off-diagonal element, respectively, associated with the NBO Fock matrix. Therefore, there is a direct relationship between F (i, j) off-diagonal elements and the orbital overlap. NBO analysis is a sufficient approach to investigate the effect of the stereoelctronic interactions on the reactivity

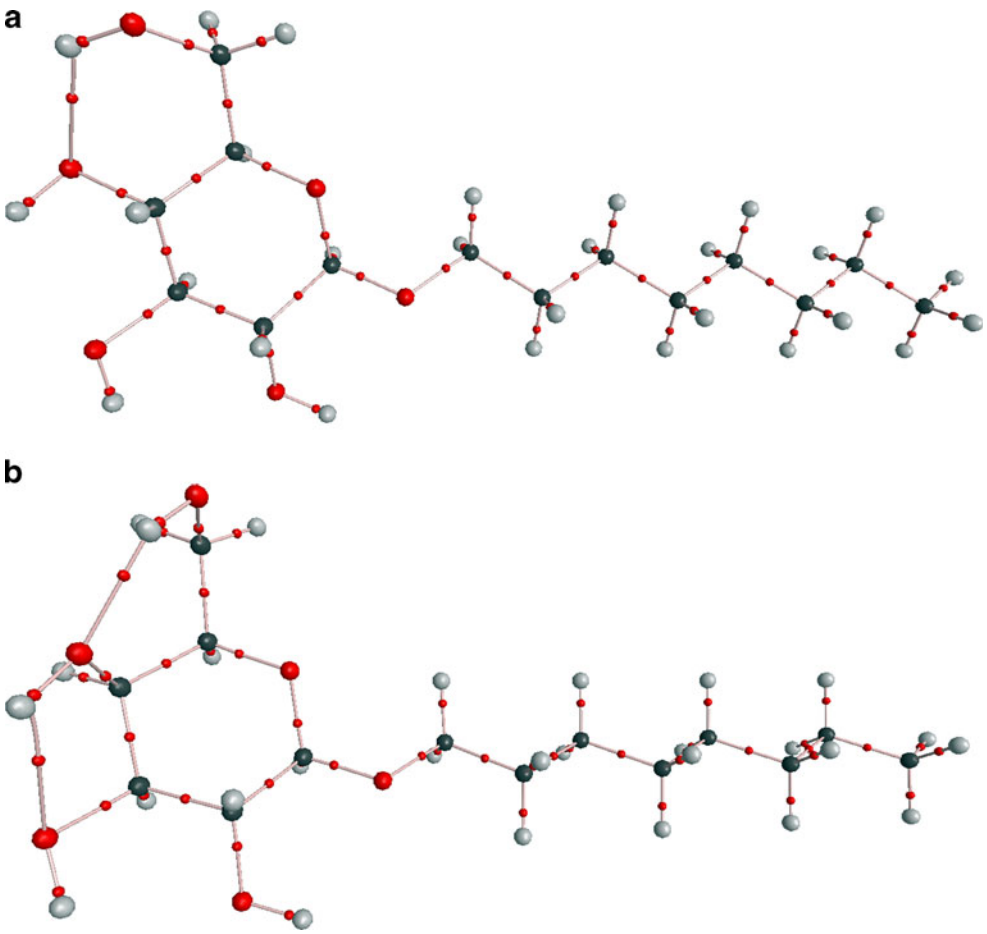

Fig. 5 Molecular graph in the **a** C_8O-β-Glc and **b** C_8O-β-Gal. Small red spheres and lines correspond to the bond critical points (BCP) and the bond paths, respectively

Table 6 The second-order perturbation energies $E^{(2)}$, (kcalmol^{-1}), corresponding to the most important charge transfer interaction (donor → acceptor) in the C_8O-β-Glc and C_8O-β-Gal by using B3LYP/6-31G level

	Donor NBO(*i*) *n*(O)	Acceptor NBO(*j*) σ*(O-H)	$E^{(2)}$ (kcalmol^{-1}) (O)→σ*(O-H)	ε_j-ε_i (a.u)	*F(i, j)* (a.u)
C_8O-β-Glc	LP(2)O4	BD*(1)HO6-O6	4.85	0.79	0.055
	LP(2)O3	BD*(1)HO4-O4	0.73	0.74	0.021
C_8O-β-Gal	LP(2)O4	BD*(1)HO6-O6	11.55	1.04	0.098
	LP(2)O3	BD*(1)HO4-O4	3.49	0.78	0.047

and dynamic behaviors of chemical compounds. The larger the $E^{(2)}$ value, the more [38] intensive is the interaction between electron donors and electron acceptors [67].

The formation of hydrogen bonds in the C_8O-β-Glc and C_8O-β-Gal implies that certain amounts of electronic charge are transferred from the lone pair to the anti–bonding orbital. Furthermore, some of the significant donor-acceptor interactions and their second order perturbation stabilization energies $E^{(2)}$, which are calculated at the B3LYP/6-31G level of theory for studied compounds, are given in Table 6. The orbital energies (ε), are reported in a.u., while the second order perturbation energies $E^{(2)}$, are reported in kcalmol^{-1}. As can be seen from Table 6, electronic charge is transferred from a lone pair orbital *n*(O) atom in donor fragment to σ*(O-H) anti-bonding orbital of the acceptor fragment. The lengthening of the O-H bond is a result of such σ*(O-H) character (HO6···O4=2.11 for C_8O-β-Glc and HO6···O4=1.85, HO3···O3 =2.09 for C_8O-β-Gal).

The stabilization energies of $E^{(2)}$ n(O) → σ*(O-H), are 4.85, 0.73 and 11.55, 3.49 (kcalmol^{-1}) in the C_8O-β-Glc and in the C_8O-β-Gal, respectively. In the C_8O-β-Glc, the charge transfer energy is smaller than that in the C_8O-β-Gal. These $E^{(2)}$ must be higher than the mentioned threshold limit for the other positions. A comparison between the NBO analysis of C_8O-β-Glc and C_8O-β-Gal shows that the value of second-order perturbation energy $E^{(2)}$ for (n_2O4 → σ*O6-HO6) is higher than the value of (n_2O3 → σ*O4-HO4). Hence, the strength of hydrogen bond in the C_8O-β-Gal is greater than that in the C_8O-β-Glc. On the other hand, we can see (Table 6) that the lowest $E^{(2)}$ value (0.73 kcal mol^{-1}) is observed for C_8O-β-Glc in (n_2O3 → σ*O4-HO4). This means that the hydrogen bond in (n_2O3 → σ*O4-HO4) is weaker than that of (n_2O4 → σ*O6-HO6). The data clearly indicates that the bonds (HO6···O4) and (HO4···O3) are favorably constructed in the C_8O-β-Gal but are almost impossible to be built in HO4···O3 in the C_8O-β-Glc. Our calculation shows that the energy gaps between HOMO and LUMO in the C_8O-β-Glc and C_8O-β-Gal are 0.49659 and 0.47510 (a.u), respectively. The calculated data are shown in Fig. 4.

In addition, the calculated wavelengths for the understudied compounds are 2497 and 2610 nm, respectively, thus falling into the short–wavelength infrared region (1400–3000) [68]. Therefore, as the results show, these materials absorb infrared frequency, which may be exploited as an infrared sensor material similar to that suggested previously for carbohydrate [69].

Conclusions

A useful tool to characterize chemical bonds is the quantum theory of atoms in molecules (QTAIM). The effects of epimerization at the C4 position of C_8O-β-Glc and C_8O-β-Gal were investigated using density functional theory. In C_8O-β-Glc, all the peripheral OH groups are equatorial, while in C_8O-β-Gal, OH4 is axial. In this current investigation, O-H distances, bond lengths, and the electronic densities at the bond critical points (BCP) were used to compare the hydrogen bond strength in C_8O-β-Glc and C_8O-β-Gal.

The results of a detailed population analysis of C_8O-β-Glc and C_8O-β-Gal by natural bond orbitals and the atoms in molecules methods can conclude as follows: the higher energy in C_8O-β-Gal compared to C_8O-β-Glc indicates that C_8O-β-Gal is more stable in forming one extra five-membered ring. The BCP calculation shows the presence of HB interaction while a further molecular graph representation shows that C_8O-β-Gal has two hydrogen bonds, and only one in C_8O-β-Glc. Hydrogen bonding of type HO6···O4 in C_8O-β-Glc and C_8O-β-Gal shows partially covalent–partially electrostatic (Pc-Pe) in nature but hydrogen bond of type HO4···O3 shows van der Waals in nature in C_8O-β-Gal. Hydrogen bonding of type HO6···O4 in both C_8O-β-Glc and C_8O-β-Gal is classified as medium and hydrogen bond type HO4···O3 in C_8O-β-Gal is classified as weak. By comparison it is apparent that hydrogen bond type HO6···O4 is much stronger than HO6···O4 in C_8O-β-Gal. IR frequencies of studied compounds fall into the short-wavelength-infrared region (1400–3000 nm). The interactions (n_2O3 → σ*HO4-O4) and (n_2O4 → σ*HO6-O6) are the most important for intramolecular interactions that play a key role in the stability of studied compounds in this work. The lowest value (0.73 kcalmol^{-1}) for C_8O-β-Glc in (n_2O3 → σ*HO4-O4), and highest value (11.55 kcalmol^{-1}) for C_8O-β-Gal in (n_2O4 → σ*HO6-O6) are observed.

Acknowledgments The authors wish to thank the UM.C/625/1/HIR-MOHE/05 grant for supporting this project and the Centre for Information Technology (PTM), University of Malaya, for providing the high performance computing facility (HPC). Discussion with professor Marek Janusz Wójcik (Jagiellonian University, Krakow, Poland) is gratefully appreciated.

References

1. Dembitsky VM (2004) Chemistry and biodiversity of the biologically active natural glycosides. Chem Biodivers 1(5):673–781. doi:10.1002/cbdv.200490060
2. Dembitsky VM (2004) Astonishing diversity of natural surfactants: 1. Glycosides of fatty acids and alcohols. Lipids 39 (10):933–953. doi:10.1007/s11745-004-1316-1
3. Brooks NJ, Hamid HAA, Hashim R, Heidelberg T, Seddon JM, Conn CE, Husseini SMM, Zahid NI, Hussen RSD (2011) Thermotropic and lyotropic liquid crystalline phases of Guerbet branched-chain-D-glucosides. Liq Cryst 38(11–12):1725–1734. doi:10.1080/02678292.2011.625689
4. Vill V, Hashim R (2002) Carbohydrate liquid crystals: structure-property relationship of thermotropic and lyotropic glycolipids. Curr Opin Colloid 7(5–6):395–409. doi:10.1016/s1359-0294(02)00091-2
5. Ahmad N, Ramsch R, Esquena J, Solans C, Tajuddin HA, Hashim R (2012) Physico-chemical charactrization of natural-like branched-chain glycosides towards formation of hexosomes and vesicles. Langmuir 28(5):2395–2403
6. Balzer D, Lüders H (2000) Nonionic surfactants: Alkyl polyglucosides. 91. CRC, Boca Raton
7. Holmberg K (2001) Natural surfactants. Curr Opin Colloid 6 (2):148–159
8. Hill K, Rhode O (1999) Sugar-based surfactants for consumer products and technical applications. Fett-Lipid 101(1):25–33
9. Jackson ML, Schmidt CF, Lichtenberg D, Litman BJ, Albert AD (1982) Solubilization of phosphatidylcholine bilayers by octyl glucoside. Biochemistry 21(19):4576–4582. doi:10.1021/bi00262a010
10. Wang J, Balazs YS, Thompson LK (1997) Solid-state REDOR NMR distance measurements at the ligand site of a bacterial chemotaxis membrane receptor†. Biochemistry 36(7):1699–1703. doi:10.1021/bi962578k
11. Harding MM, Anderberg PI, Haymet ADJ (2003) 'Antifreeze' glycoproteins from polar fish. Eur J Bio Chem 270(7):1381–1392. doi:10.1046/j.1432-1033.2003.03488.x
12. Varki A (1993) Biological roles of oligosaccharides: all of the theories are correct. Glycobiology 3(2):97–130. doi:10.1093/glycob/3.2.97
13. Israelachvili J (1994) The science and applications of emulsions—an overview. Colloid Surf A 91:1–8. doi:10.1016/0927-7757(94)02743-9
14. Helm CA, Israelachvili JN, McGuiggan PM (1992) Role of hydrophobic forces in bilayer adhesion and fusion. Biochemistry 31 (6):1794–1805. doi:10.1021/bi00121a030
15. Emsley J (1980) Very strong hydrogen bonding. Chem Soc Rev 9 (1):91–124. doi:10.1039/CS9800900091
16. Claesson PM, Kjellin M, Rojas OJ, Stubenrauch C (2006) Short-range interactions between non-ionic surfactant layers. Phys Chem Chem Phys 8(47):5501–5514. doi:10.1039/B610295F
17. Larson JW, McMahon TB (1984) Gas-phase bihalide and pseudobihalide ions. An ion cyclotron resonance determination of hydrogen bond energies in XHY- species (X, Y = F, Cl, Br, CN). Inorg Chem 23(14):2029–2033. doi:10.1021/ic00182a010
18. Jeffrey GA, Saenger W (1994) Hydrogen bonding in biological structures. Springer, Berlin
19. French AD, Brady JW (1990) Computer modeling of carbohydrates. Am Chem Soc 430. doi:10.1021/bk-1990-0430.ch001
20. Fringant C, Tvaroska I, Mazeau K, Rinaudo M, Desbrieres J (1995) Hydration of α-maltose and amylose: molecular modelling and thermodynamics study. Carbohyd Res 278(1):27–41. doi:10.1016/0008-6215(95)00232-1
21. Brady JW, Schmidt RK (1993) The role of hydrogen bonding in carbohydrates: molecular dynamics simulations of maltose in aqueous solution. J Phys Chem 97(4):958–966. doi:10.1021/j100106a024
22. Chong TT, Heidelberg T, Hashim R, Gary S (2007) Computer modelling and simulations of thermotropic and lyotropic alkyl glycoside bilayers. Liq Cryst 34(3):349–363. doi:10.1080/02678290601111556
23. Arunan E, Desiraju G, Klein R, Sadlej J, Scheiner S, Alkorta I, Clary D, Crabtree R, Dannenberg J, Hobza P (2010) Definition of the Hydrogen Bond(IUPAC Recommendation). Pure Appl Chem 83(8):1637–1641. doi:10.1351/PacRec-10-01-02
24. Bader RFW (1991) A quantum theory of molecular structure and its applications. Chem Rev 91(5):893–928. doi:10.1021/cr00005a013
25. Bader R, Essen H (1984) The characterization of atomic interactions. J Chem Phys 80:1943-1960
26. Arnold WD, Oldfield E (2000) The chemical nature of hydrogen bonding in proteins via NMR: j-couplings, chemical shifts, and AIM theory. J Am Chem Soc 122(51):12835–12841. doi:10.1021/ja0025705
27. Espinosa E, Molins E, Lecomte C (1998) Hydrogen bond strengths revealed by topological analyses of experimentally observed electron densities. Chem Phys Lett 285(3–4):170–173
28. Grabowski SJ (2001) A new measure of hydrogen bonding strength-*ab initio* and atoms in molecules studies. Chem Phys Lett 338(4–6):361–366. doi:10.1016/S0009-2614(01)00265-2
29. Ikushima Y, Hatakeda K, Saito N, Arai M (1998) An in situ Raman spectroscopy study of subcritical and supercritical water: the peculiarity of hydrogen bonding near the critical point. J Chem Phys 108:5855–5860
30. Ionescu AR, Bérces A, Zgierski MZ, Whitfield DM, Nukada T (2005) Conformational pathways of saturated six-membered rings. A static and dynamical density functional study. J Phys Chem A 109(36):8096–8105. doi:10.1021/jp052197t
31. Barnett CB, Naidoo KJ (2008) Stereoelectronic and solvation effects determine hydroxymethyl conformational preferences in monosaccharides. J Phys Chem B 112(48):15450–15459
32. Grabowski SJ (2001) *Ab Initio* calculations on conventional and unconventional hydrogen bondsstudy of the hydrogen bond strength. J Phys Chem A 105(47):10739–10746. doi:10.1021/jp011819h
33. Gilli P, Bertolasi V, Ferretti V, Gilli G (1994) Covalent nature of the strong homonuclear hydrogen bond. Study of the OH–-O system by crystal structure correlation methods. J Am Chem Soc 116(3):909–915
34. Mó O, Yáñez M, Elguero J (1992) Cooperative (nonpairwise) effects in water trimers: an *ab initio* molecular orbital study. J Chem Phys 97:6628–6638
35. Vill V (2006) The stereochemistry of glycolipids. A key for understanding membrane functions? Liq Cryst 33(11–12):1351–1352. doi:10.1080/02678290601140571
36. Espinosa E, Souhassou M, Lachekar H, Lecomte C (1999) Topological analysis of the electron density in hydrogen bonds. Acta Crystallogr Sec B 55(4):563–572. doi:10.1107/S0108768199002128
37. Weinhold F (1997) Nature of H-bonding in clusters, liquids, and enzymes: an *ab initio*, natural bond orbital perspective. J Mol Struct 398–399:181–197. doi:10.1016/S0166-1280(96)04936-6

38. Reed AE, Curtiss LA, Weinhold F (1988) Intermolecular interactions from a natural bond orbital, donor-acceptor viewpoint. Chem Rev 88(6):899–926. doi:10.1021/cr00088a005
39. Becke AD (1993) Density-functional thermochemistry. III. The role of exact exchange. J Chem Phys 98(7):5648–5652. doi:10.1063/1.464913
40. Lee C, Yang W, Parr RG (1988) Development of the Colle-Salvetti correlation-energy formula into a functional of the electron density. Phys Rev B 37(2):785–789
41. Ditchfield R, Hehre W, Pople JA (1971) Self-consistent molecular-orbital methods. IX. An extended Gaussian-type basis for molecular-orbital studies of organic molecules. J Chem Phys 54:724
42. Francl MM, Pietro WJ, Hehre WJ, Binkley JS, Gordon MS, DeFrees DJ, Pople JA (1982) Self-consistent molecular orbital methods. XXIII. A polarization–type basis set for second–row elements. J Chem Phys 77(7):3654–3665. doi:10.1063/1.444267
43. Miertus S, Scrocco E, Tomasi J (1981) Electrostatic interaction of a solute with a continuum. A direct utilizaion of ab initio molecular potentials for the prevision of solvent effects. Chem Phys 55(1):117–129
44. Frisch MJ, Trucks GW, Schlegel HB et al (2009) Gaussian 09, Revision A. 02. Wallingford CT
45. Dennington R, Keith T, Millam JGV (2008) Version 5.0. 8. Semichem Inc, Shawnee Mission, KS
46. Bader R (1995) Atoms in molecules. A quantum theory. Oxford University Press, Oxford
47. Popelier P (2000) Atoms in molecules. An introduction. Prentice Hall
48. Biegler-König F, Schönbohm J, Derdau R, Bayles D, Bader R (2002) AIM2000, version 2.0. University of Applied Sciences, Bielefeld
49. Glendening E, Reed A, Carpenter J, Weinhold F (2003) NBO 3.1
50. Schuster P, Zundel G, Sandorfy C (1976) Hydrogen bond; recent developments in theory and experiments. North-Holland, Amsterdam
51. Pimentel GC, McClellan AL (1960) The hydrogen bond. Freeman, San Francisco
52. Momany FA, Appell M, Willett JL, Schnupf U, Bosma WB (2006) DFT study of α- and β-d-galactopyranose at the B3LYP/6-311++G** level of theory. Carbohyd Res 341(4):525–537
53. Panico R, Powell WH, Richer JC (1993) A guide to IUPAC nomenclature of organic compounds: recommendations 1993. International Union of Pure Applied Chemistry. Commission on the Nomenclature of Organic Chemistry. Blackwell Scientific, Oxford
54. Momany FA, Appell M, Willett JL, Bosma WB (2005) B3LYP/6-311++G** geometry-optimization study of pentahydrates of a- and b-D-glucopyranose. Carbohyd Res 340:1638–1655
55. Appell M, Willett JL, Momany FA (2005) DFT study of α- and β-d-mannopyranose at the B3LYP/6-311++G** level. Carbohyd Res 340(3):459–468
56. Silvestrelli PL, Parrinello M (1999) Water molecule dipole in the gas and in the liquid phase. Phys Rev Lett 82(16):3308–3311
57. Parr RG, Lv S, Liu S (1999) Electrophilicity index. J Am Chem Soc 121(9):1922–1924. doi:10.1021/ja983494x
58. Ortiz EV, López MB (2007) Density Functional Theory (DFT) applied to the study of the reactivity of platinum surface modified by nickel nanoparticles. Mec Comp 26:1692
59. Pearson RG, Pearson R (1997) Chemical hardness: applications from molecules to solids. Wiley-VCH, Weinheim
60. Parr RG, Zhou Z (1993) Absolute hardness: unifying concept for identifying shells and subshells in nuclei, atoms, molecules, and metallic clusters. Acc Chem Res 26(5):256–258. doi:10.1021/ar00029a005
61. Pearson RG (1988) Absolute electronegativity and hardness: application to inorganic chemistry. Inorg Chem 27(4):734–740. doi:10.1021/ic00277a030
62. Pearson RG (1987) Recent advances in the concept of hard and soft acids and bases. J Chem Edu 64(7):doi:10.1021/ed064p561
63. Bader RFW (1990) Atoms in molecules-a quantum theory. Oxford University Press, New York
64. Popelier P, Bader R (1992) The existence of an intramolecular C-H… O hydrogen bond in creatine and carbamoyl sarcosine. Chem Phys Lett 189(6):542–548. doi:10.1016/0009-2614(92)85247-8
65. Popelier PLA (1998) Characterization of a dihydrogen bond on the basis of the electron density. J Phys Chem A 102(10):1873–1878. doi:10.1021/jp9805048
66. Nazari F, Doroodi Z (2010) The substitution effect on heavy versions of cyclobutadiene. Int J Quantum Chem 110(8):1514–1528. doi:10.1002/qua.22271
67. Reed AE, Weinhold F (1985) Natural localized molecular orbitals. J Chem Phys 83(4):1736–1740
68. Henderson R (2007) Wavelength considerations. Instituts für Umform-und Hochleistungs. Archived from the original on:10–28
69. Amerov A, Chen J, Arnold M (2004) Molar absorptivities of glucose, water and other biological molecules over the first overtone and combination regions of the near infrared spectrum. Appl Spect J 58:1195–1204